

Dynamics of the West African Westerly Jet

Bing Pu¹ and Kerry H. Cook²

¹ Department of Earth and Atmospheric Sciences, Cornell University, Ithaca NY, 14853

² Department of Geological Sciences, Jackson School of Geosciences, The University of Texas at Austin, Austin, TX, 78712

I Introduction

It has long been recognized that the low-level flow across the West Coast of Africa from the tropical North Atlantic plays a major role in transporting moisture into the Sahel during the summer, and it is important for rainfall variability on all time scales (e.g., Grist and Nicholson 2001, Patricola and Cook 2007). This low-level flow was identified as a low-level jet in satellite-based observations and discussed as an ocean-based dynamical feature within the Atlantic ITCZ (Grodsky and Carton 2003). Here we examine the details of the jet's dynamics and the processes that cause the jet to form. Our study distinguishes the jet from the westerly acceleration of the West African monsoon flow across the Guinean Coast, suggesting that this jet provides a separate source of moisture flux into the Sahel. The structure, seasonality, diurnal cycle, and dynamics of the jet are investigated using the high resolution ERA40 reanalysis (320 x 160 Gaussian Latitude/Longitude), with the lower resolution NCEP/DOE AMIP-II reanalysis added for reference (Figure 1).

West African westerly jet (WAWJ)

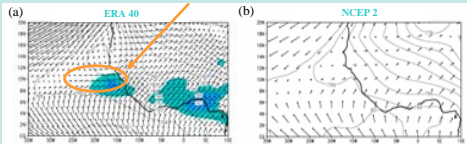


Figure 1. 925 hPa winds and geopotential heights in the (a) ERA 40 climatology and (b) NCEP2 climatology, averaged from June 1st to September 30th. Zonal wind speeds larger than 4 m/s are shaded with light blue, and above 5 m/s with dark blue.

II The low-level jet in the reanalysis

Based on daily zonal wind speed variations in the ERA40 reanalysis at 925hPa, the level at which the jet is strongest, five stages of jet development are identified (Figure 2). The westerly jet forms over the ocean close to the east coast of north Africa in early June, then expands westward over the Northern Atlantic. It reaches a maximum during late July and early September with peak wind speeds around 6-7m/s in the climatology, and retreats and fades in mid October.

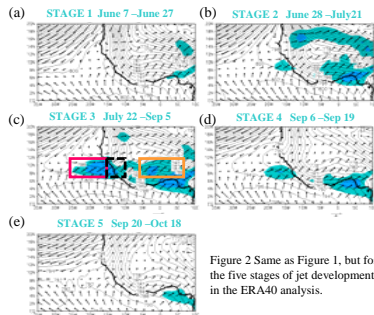


Figure 2 Same as Figure 1, but for the five stages of jet development in the ERA40 analysis.

Examining the vertical structure of the WAWJ helps distinguish this circulation feature from that of the monsoon flow, which is southwesterly across the Guinean Coast and turns more westerly inland due to Coriolis accelerations. As seen in Figures 3a-b, westerly flow occupies the lower troposphere from 1000 hPa to about 700 hPa over West Africa. In the latitudinal cross section (Fig. 3a), the WAWJ is centered at 9°N and 925 hPa. It is clear in the longitudinal cross section (Fig. 3b) that the WAWJ forms a distinct core near 17°W, and the region is characterized by upward vertical velocities. In contrast, the westerly monsoon flow is basically horizontal without an organized core region.

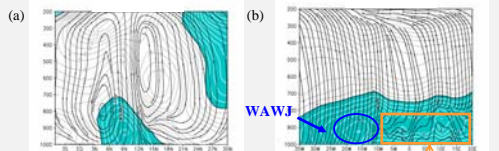
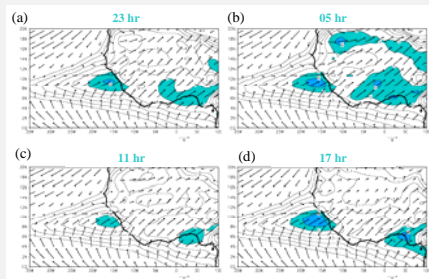


Figure 3. Cross-sections of the zonal wind speed (westerlies are shaded) with (a) streamlines of meridional and vertical winds (scaled by 10³) averaged over 15°W-25°W and (b) streamlines of zonal and vertical winds averaged over 8.4°-10.6°N, averaged from July 22nd to September 5th.

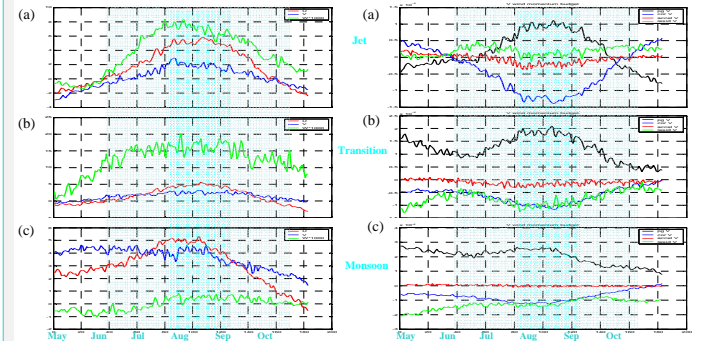


Figures 4a-d Climatological 6-hourly wind vectors and zonal wind speed at 925 hPa during the jet maximum (July 22 - September 5) at 23 hr, 05 hr, 11 hr and 17 hr local time, respectively. The contours are westerly wind speeds, with blue and dark blue shadings indicating wind speed above 5 m/s and 6 m/s, respectively

In the 6-hourly ERA40 climatology, the westerly jet displays a weak diurnal cycle with strongest winds at 17 hr and weakest at 11 hr local time. The amplitude of the diurnal cycle is about 1-2 m/s.

III Dynamics of the westerly jet

A momentum budget analysis is applied in the vicinity of the jet, in the West African monsoon region, and the transition region that separates them (see the boxes in Fig. 2c). As the Coriolis force is a little larger than the pressure gradient force, the resultant ageostrophic winds are positive and the jet is supergeostrophic. The ageostrophic westerly wind is about 1-1.5 m/s at jet maximum. In both the transition and monsoon regions, the meridional pressure gradient is about as twice large as in the jet region and cannot be balanced by the Coriolis force, so the actual wind speeds are subgeostrophic with the ageostrophic easterly winds of about 5-6 m/s in July-August.



Figures 5a-c Averaged wind speeds (m/s) in the jet (15°-25°W), transition (10°-15°W) and monsoon (5°W-5°E) regions at the same latitudes (8.4°-11.6°N). In the jet region, the average zonal winds are the strongest among the three but the meridional winds are weak. While in the monsoon region the zonal wind and meridional wind speeds are comparable. The jet region is also distinguished from the monsoon region by the strong vertical winds, as also shown in Fig. 3. Between the two regions there is a transition region with even stronger vertical velocities.

Figure 6. Meridional momentum budgets in the (a) jet, (b) transition, and (c) monsoon regions.

$$\frac{\partial v}{\partial t} + u \frac{\partial v}{\partial x} + v \frac{\partial v}{\partial y} + \omega \frac{\partial v}{\partial p} = -\frac{\partial \phi}{\partial y} - 2\Omega u \sin \phi + R$$

$\text{accel}V$ $\text{cor}V$ $\text{resid}V$

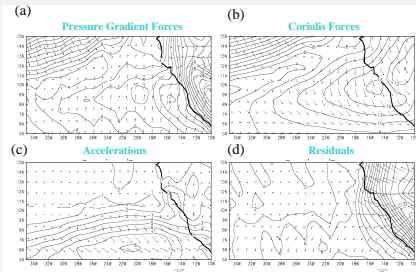


Figure 7 Vectors and magnitudes of main terms in the momentum equation, averaged over the time of jet maximum: (a) pressure gradient forces; (b) Coriolis forces; (c) acceleration term (dv/dt); (d) residual. The vectors are the composites of the meridional and zonal components of each term, while the contours are the magnitudes of the composites. All the values are scaled by 10³.

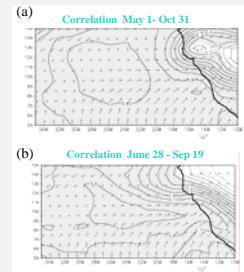


Figure 8. Correlation distribution of the averaged zonal wind speed in the jet region (8.4°-10.6°N, 15°-25°W) and meridional pressure gradient forces at 925 hPa for (a) May 1st - Oct. 31st and (b) Jun. 28th - Sep. 19th. Wind vectors are averaged in jet maximum stage. Shading denotes 95% confidence level.

As shown in Fig. 7a-b, at jet maximum, northward pressure gradient forces and the southward Coriolis forces are the biggest terms among the four at the jet region. The accelerations are mainly meridional and increase southward. The residuals are similar in magnitude to the acceleration term in 8.4°-9.5°N, but are twice as strong in the north and an order of magnitude larger over land.

Figure 8 shows that the zonal wind speeds in the jet region are highly correlated to the meridional pressure gradient in the region of 8°-13°N over the ocean in both the seasonal cycle and during the jet maximum period.

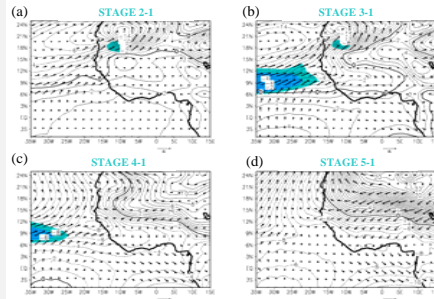


Figure 9 Geopotential heights and wind anomalies at stages 2-5, with reference to stage one.

As revealed in Figure 9, in the jet developing stages 2 and 3, the pressure gradient intensifies in the jet region as pressures fall in the north and rise in the south. The resulting northward pressure gradient force causes the geostrophic westerly wind anomaly associated with the WAWJ. After stage 4, pressure gradients north of the jet become westward instead of southward, and to the south the pressures fall. As the meridional pressure gradient anomaly decreases, the westerly wind anomaly decreases and finally disappears.

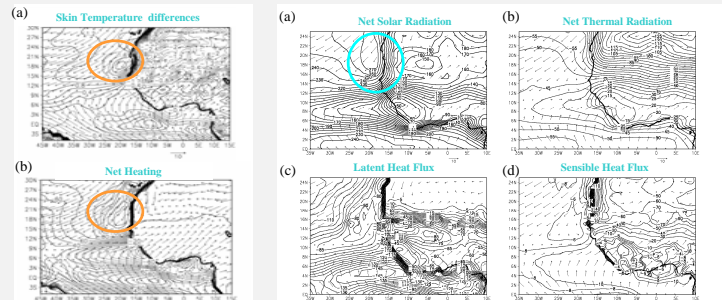


Figure 10. (a) Skin temperature differences (K) (Sep 5th minus July 22nd) and (b) surface net heating (W/m²) averaged between July 22nd and Sept 5th. Vectors are winds at 925 hPa, averaged during the jet maximum.

Figure 11 Radiation budgets (W/m²) at the surface in the ERA40 reanalysis. (a) Net downward solar radiation. (b) Net upward thermal radiation. (c) Upward latent heat flux. (d) Upward sensible heat flux. Vectors are winds at 925 hPa, averaged during jet maximum.

As shown in Figure 10a, from July 22nd to September 5th, SST increases by more than 1.2K to the north of the WAWJ at 15°-25°N. The warming SST is the main contributor to the development of the local low at 925 hPa that supports the jet. Figure 10b suggests that the SST warming is caused by the surface net downward heating in the region during the period. Details about the radiation budgets are shown in Figure 11. The localized ocean warming is related to the downward net solar heating, which is closely related to the cloud distribution over the ocean.

IV Conclusions and Future Work

- The low-level westerly jet over West Africa starts at the beginning of June, reaches its maximum during August, and fades at mid October. According to the strength of the zonal wind speed, five stages of jet development have been identified in ERA 40 daily climatology reanalysis.
- During jet peak time, it covers the region of 17°-30°W and 8°-11°N. The maximum zonal wind speed reaches 7 m/s at 925 hPa in the ERA40 reanalysis.
- The low-level westerly jet is geostrophic to first order, and we have identified pressure variations between 5°-15°N over the ocean that are associated with its formation. A local low at 925 hPa is the main contributor to the meridional pressure gradient in the jet region.
- At jet maximum, the local low is mainly maintained by ocean surface heating, which is mainly caused by net solar radiative heating at 15°-20°N. At the beginning stage of jet formation, the meridional advection of warm air from the north may also contribute to local low formation, but future work will clarify the processes of jet formation.
- The jet is supergeostrophic. Future work will concentrate on investigating the momentum budget in more detail, understanding in particular the role of frictional accelerations and their changes across the west coast of Africa.

References

Grist, J. P., and S. E. Nicholson, 2001: A study of the dynamic factors influencing the rainfall variability in the West African Sahel. *J. Climate*, **14**, 1337-1359.

Patricola, C.M., and K. Cook, 2007: Dynamics of the West African Monsoon under Mid-Holocene Precessional Forcing: Regional Climate Model Simulations. *J. Climate*, **20**, 694-716.

Grodsky, S. A., J. A. Carton, and S. Nigam, 2003: Near surface westerly wind jet in the Atlantic ITCZ. *Geophys. Res. Lett.*, **30**, 1-4.

UCAR/NCAR/CISL/DSS and ECMWF, 2005: ERA40 T106 Analysis Fields on Pressure Surfaces, created at NCAR. Published by the *CISL Data Support Section at the National Center for Atmospheric Research, Boulder, CO* (ds127.1).

UCAR/NCAR/CISL/DSS and ECMWF, 2005: ERA40 T106 6-hourly Surface Analysis and Surface Forecast Fields, created at NCAR. Published by the *CISL Data Support Section at the National Center for Atmospheric Research, Boulder, CO* (ds127.0).